QUANTITATIVE MICROANALYSIS EXPLORER: NEXT-GENERATION TOOL FOR ANALYSIS OF APOLLO 17 CORE 73002,6015-6018. P.K. Carpenter[1], R.C. Ogliore[2], A. Minocha[2], C. J-K. Yen[1], B.L. Jolliff[1], and the ANGSA Science Team, which includes the JSC curation team. [1]Dept. of Earth and Planetary Sciences (paulc@wustl.edu), [2]Dept. of Physics and [1,2]McDonnell Center for the Space Sciences, Washington University, St. Louis, MO, USA.

Introduction: The *Quantitative Microanalysis Explorer* (QME) is a web-based tool developed to analyze Apollo 17 core samples 73002,6015-6018 [1,2]. The QME combines optical microscope images (reflected, transmitted, and crossed-polars) with backscattered-electron, X-ray intensity, and quantitative EPMA map data. The QME provides a framework for convenient evaluation of texture and mineral chemistry, and enables diverse researchers without direct access to the samples to conduct web-based petrologic analysis.

Electron Microprobe Imaging and Quantitative Compositional Mapping: Polished thin sections (PTS) of 73002 continuous core are distributed as 50 × 25 mm epoxy grain mounts of regolith. Mosaic optical image maps of these PTS were obtained using the Keyence automated optical microscope system at JSC. The PTS were subsequently mapped using the JEOL JXA-8200 electron microprobe (EPMA) at Washington University. Approximately 325 beam-raster backscattered-electron (BSE) images were acquired at 15 kV and 2 nA probe current at 70× magnification, and stitched using the ImageJ Fiji grid-collection stitching plug-in [3], to produce a 20k by 5k BSE mosaic base map with ~ 1.5 μm pixel resolution. For each 73002 slide, five EPMA stage maps were acquired using fixed wavelength-dispersive spectrometers (WDS). Each stage map was acquired at 1024 × 1024 resolution using a step size of 9.5 μm with a fixed 10 μm electron beam at 15 kV and 100 nA probe current using a dwell time of 25 msec. Two passes were used to collect X-ray intensities for Mg, Al, Fe, Ca, and Ti in pass 1, and Na, Si, Mn, K, and Cr in pass 2, with a total acquisition time of 18 hrs. per map.

The X-ray intensity maps were processed using Probe Software CalcImage and Probe for EPMA, by performing a full Φ(ρz) correction at each pixel [4]. This correction is of the form C = k × ZAF, where *C* is the element concentration, the k-ratio $k = (P\text{-}B)^{smp}/(P\text{-}B)^{std}$ is the background corrected relative peak X-ray intensity (P-B) at each pixel in the map compared to the calibration standard, and *ZAF* is the compositionally dependent matrix correction for atomic number *Z*, X-ray absorption *A*, and characteristic fluorescence *F* in both the sample and standard.

The Φ(ρz) correction uses a standards-based mean atomic number (MAN) background calibration which is accurate and internally-consistent, and allows all map collection time to be dedicated to on-peak X-ray measurement [4]. This improves precision and results in detection limits of ~ 0.1 – 0.2 element wt.%.

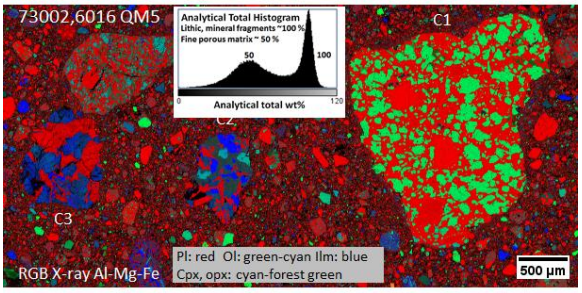

Figure 1. Al-Mg-Fe RGB X-ray map showing clasts 1, 2, and 3 from 73002,6016 quant map 5. Plagioclase is red, olivine and pyroxene are green-blue depending on Mg:Fe. Inset shows analytical total histogram for this map area.

The result is a full quantitative analysis at each pixel. Matlab routines are used to write for each element a 32-bit floating point .tiff file, which results in files for element and oxide wt.%, cation stoichiometry, derived mineral end member maps, and input image stacks for ENVI processing [5]. These maps were stitched using Fiji and Matlab routines and registered to the BSE base maps for each PTS. For the 73002 core PTS this results in a total of approximately 2.1×10^7 EPMA analyses.

Quantitative Microanalysis Explorer Web Tool: The stitched mosaic optical and compositional maps are quite large and inspection of the EPMA analysis data requires a tool to reconstruct the analysis from the individual element files. The QME tool uses OpenSeadragon to browse the images with rapid zoom and pan capabilities, and Javascript routines are used to retrieve EPMA data for single point and both regular and irregular polygon regions [2]. The tool allows extraction of element, oxide, and cation formula data for these discrete point and polygon regions as outlined by the mouse. This extracted EPMA data is automatically copied to the clipboard for pasting into applications such as Excel.

Co-registration of the optical and X-ray/quant map data is made relative to the BSE base map. For a given field of view of the PTS one can switch between optical, BSE, and X-ray image sources. An Al-Mg-Fe RGB composite X-ray map in Fig. 1 shows feldspathic material in red, forsteritic olivine in bright green, and ferroan olivine in cyan. Pyroxenes are blue to forest green for orthopyroxene, depending on Mg:Fe, and dark green in Ca pyroxene due to Al and Ti substitution.

Discussion and Example: The compositional mapping data for 73002 is of high analytical quality. The core samples include large lithic and mineral fragments

as well as fine submicron particles. The analytical total histogram for 73002,6016 QM5 (Fig. 1) illustrates normal totals of ~100 wt.% for larger well-polished fragments, and totals of ~ 50 wt. % for fine-grained matrix fragments embedded in casting epoxy.

In Fig. 1, clast C1 is a troctolitic granulite breccia consisting of unzoned olivine, plagioclase with variable Na content, and minor Cpx, Opx, and armalcolite. Table 1 demonstrates the high analytical quality of QME data extracted from an inscribed rectangular polygon (n=391 pixels) compared to conventional EPMA spot analyses (n=20) measured on several olivine crystals. This comparison highlights the nature of spot analysis (high analytical quality and few in number) with mapping results (historically low analytical quality but high in number) Using the QME tool, we observe that single pixel and small region selections allow mineral identification, detection of chemical zoning, and comparison of different clasts. Larger region selections provide better averages owing to the greater number of pixels sampled.

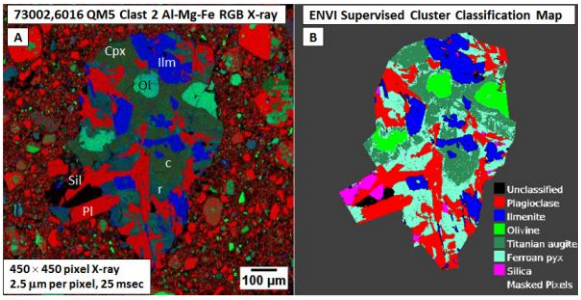

Figure 2A: High-Ti basalt clast C2, Al-Mg-Fe RGB X-ray map. Ca-pyroxene cores c have elevated Ti, Al, Cr, and Ca; rims r have elevated Mg, Fe, and Si. **Figure 2B:** ENVI classification map used for bulk analysis calculation.

In Fig. 1, C2 is a 0.5 × 1.0 mm high-Ti basalt clast. As seen in Fig. 2A Al-Mg-Fe RGB image, this clast contains plagioclase, ilmenite, olivine, silica, and zoned Ca-pyroxene. Compositions of these phases were determined by EPMA spot analysis, and rectangular polygon extraction using QME (Table 2A). ENVI was used to determine the modal proportions of these phases using supervised cluster analysis, and the classification map is shown in Fig 2B. These modal proportions have been used to calculate a density-corrected bulk composition for the high-Ti basalt. Table 2B compares the bulk calculation based on mineral compositions using EPMA, QME, and ENVI.

These results illustrate several points. First, the QME and ENVI data are of comparable accuracy to EPMA spot analyses, demonstrating the high analytical quality of each. Second, there is an increase in sampling coverage from the EPMA, QME, and ENVI data with full coverage of all pixels represented by the ENVI calculation. Because ENVI classifies all pixels in a defined phase, boundary pixels with mixed composition are included which affects minor and trace element compositions. Finally, these results show a very similar composition compared to the 1974 Rose bulk analysis of ilmenite basalt 70017 [7], which demonstrates the capability to quantitatively compare microchemistry with bulk chemistry. In comparison, the sampled cross-section of clast C2 likely has lower modal ilmenite, higher plagioclase, and less ferroan olivine and Ca-pyroxene compared to 70017.

We are using the QME tool to analyze 73002 core and clast chemistry in the search for Tycho ejecta fragments [8,9], identification of pyroclastic glass spherules [10], and petrology of VLT basalt clast 73002,455 [11].

Summary: We discuss significant advances in quantitative EPMA compositional mapping, demonstrate the capabilities of the QME web tool for extraction of data, and apply these methods to the 73002,6015-6018 sections. This set of research tools provides a framework for rapid inspection of materials in the 73002 core and a comprehensive approach to compositional mapping.

Table 1. Comparison of EPMA with QME data for olivine in clast C1 troctolitic assemblage of Fig. 1.

Table 1	SiO_2	TiO_2	Al_2O_3	Cr_2O_3	FeO	MnO	MgO	CaO	Na_2O	K_2O	Total
EPMA N=20	39.85	0.09	0.02	0.14	14.19	0.16	45.95	0.09	0.00	0.00	100.47
QME N=391	39.02	0.10	0.25	0.15	15.62	0.19	45.76	0.21	0.07	0.03	99.50

Table 2A. High-Ti basalt clast C2, QME mineral compositions.
Table 2B. Bulk composition recalculation of high-Ti basalt clast C2 using ENVI modal proportions using mineral compositions by EPMA, QME, and ENVI.

Table 2A: QME Mineral Compositions						Table 2B: Bulk Recalculation			
	Plag n=30	Ilm n=36	Ol n=16	Cpx Core n=42	Cpx Rim n=35	EPMA	QME	ENVI	70017 Rose 1974
SiO_2	47.88	2.07	35.96	45.16	49.06	39.16	38.97	38.18	38.80
TiO_2	0.31	49.95	0.31	4.03	1.65	11.90	11.28	12.14	12.84
Al_2O_3	31.42	1.54	0.18	6.38	2.07	9.06	9.11	9.11	8.54
Cr_2O_3	0.04	2.17	0.22	0.79	0.34	0.36	0.72	0.44	0.49
FeO	1.31	42.1	28.91	9.44	17.2	17.96	17.24	18.17	18.12
MnO	0.11	0.44	0.4	0.21	0.26	0.27	0.25	0.37	0.24
MgO	0.43	2.61	32.94	12.78	14.12	9.56	9.54	9.57	10.16
CaO	17.02	0.45	0.61	18.55	14.79	11.40	12.03	11.45	10.56
Na_2O	1.47	0.12	0.04	0.11	0.05	0.37	0.38	0.48	0.33
K_2O	0.11	0.07	0.01	0.04	0.03	0.01	0.06	0.09	0.07
Total	100.09	101.51	99.58	97.49	99.57	100.04	99.59	100	100.15

Acknowledgements: We thank NASA for loan of the 73002 drive tube continuous core thin sections and for funding via the ANGSA Program (80NSSC19K0958).

References: [1] Carpenter P. et al. (2022) *A17-ANGSA Workshop #2031*; [2] Minocha A. et al. (2022) *A17-ANGSA Workshop #2019*; [3] Fiji url link; [4] Donovan J. et al. (2021) Am. Mineral. 106 (11) 1717-1735; [5] Harris geospatial link;[7] JSC curator 70017 link;[8] Jolliff B.L. et al. (2022) *A17-ANGSA Workshop #2043*; [9] Jolliff B.L. et al. (2023) *#1818* ;[10] Yen C.K. et al (2022) *A17-ANGSA Workshop #2010*; [11] Yen C.K. et al. (2023) *This Conference*.